



A new ginger extract characterization: Immunomodulatory, antioxidant effects and differential gene expression

Roberta Russo^{a,*}, Maria Assunta Costa^b, Nadia Lampiasi^a, Marco Chiaramonte^a, Alessia Provenzano^b, Maria Rosalia Mangione^b, Rosa Passantino^b, Francesca Zito^a

^a Consiglio Nazionale delle Ricerche, Istituto per la Ricerca e l'Innovazione Biomedica, Via Ugo La Malfa 153, 90146, Palermo, Italy

^b Consiglio Nazionale delle Ricerche, Istituto di Biofisica, Via Ugo La Malfa 153, 90146, Palermo, Italy

ARTICLE INFO

Keywords:

mRNA expression
Inflammation
Bioactive molecules
Cytokines
RAW264.7 cells

ABSTRACT

Ginger (*Zingiber officinale*) is commonly consumed as spice or herbal medicine with anti-inflammatory, antioxidant, and anticancer properties. It is rich of many bioactive constituents, mainly gingerols and shogaols. Although the bioactive constituents have been identified, the molecular mechanisms of ginger action are still limited, and the related signalling pathways not completely defined. Here, we used a simple ethanol/freeze-drying method to obtain a new ginger extract (GE), which was chemically characterised by Folin-Ciocalteu, antioxidant ORAC and HPLC assays. At cellular level, anti-inflammatory/antioxidant properties of GE, in addition to the commercial [6]-gingerol, were evaluated using RAW264.7 murine macrophages. Cell viability tests verified the non-toxic doses of GE and [6]-gingerol, and the glutathione assay confirmed the antioxidant property of GE. By quantitative PCR, we analysed the differential expression of various genes in LPS-treated cells, after GE/[6]-gingerol pre-treatments. The genes belonged to different categories: immune signalling, pro-/anti-inflammatory cytokines, pro-/anti-oxidant enzymes, hallmarks of macrophage polarization and endoplasmic reticulum stress response. Results showed that pre-treatment with two doses of GE reduced the LPS-induced expression of TLR4, MyD88, Rel-A, IL-1 α , IL-6, TNF- α , IL-10, iNOS and TRIB3 genes to varying degrees, whereas increased Jun, Light/Tnfsf14, HO-1 and Arg-1 gene expression. No effect was found on MIF expression in LPS-induced cells after GE pre-treatments. These results also suggested that GE pre-treatment promotes the expression of specific markers of macrophage polarization in LPS-stimulated cells, with a trend to activate an anti-inflammatory M2 phenotype. Further analyses will broaden the understanding of the role of individual GE components in cellular inflammation/immunomodulation.

1. Introduction

Nowadays, there is a growing interest in the use of medicinal plants for health care due to their various health-promoting effects, including prevention and/or synergistic effects with drugs in the treatment of cancer. Moreover, the reduced side effects, their availability and accessibility, and the reduced costs of production are further attractive features. Many studies have reported the presence of several bioactive compounds among the medicinal plants components, well known for their anti-inflammatory and/or immunomodulatory activities (Serrano et al., 2018).

Zingiber officinale Roscoe (Zingiberaceae), known as ginger, is a tropical monocotyledon plant with a perennial tuberous rhizome, commonly used as a spice in African, American and Chinese populations,

although it is extensively used also in western cuisine. For centuries, ginger has also been used in the traditional medicine for the treatment of many diseases and health disorders, like nausea, loss of appetite, asthma, cough, palpitation, inflammation (Mozaffari-Khosravi et al., 2014). Recently, different pharmacological properties have been ascribed to ginger and its derivatives, including antioxidant, anti-inflammatory, immunomodulatory, anticancer (Ballester et al., 2022; Mao et al., 2019b; Mashadi NS et al., 2013).

The overproduction of free radicals, such as reactive oxygen species (ROS), indicating an oxidative stress, is known to play a key role in the development of many chronic diseases (Mazahery et al., 2019; Poprac et al., 2017). Ginger and its bioactive compounds appear to have a protective effect against oxidative stress. It should be emphasized, however, that the antioxidant activity of ginger is affected by different

* Corresponding author.

E-mail address: roberta.russo@irib.cnr.it (R. Russo).

<https://doi.org/10.1016/j.fbio.2023.102746>

Received 5 April 2023; Received in revised form 10 May 2023; Accepted 12 May 2023

Available online 20 May 2023

2212-4292/© 2023 The Authors. Published by Elsevier Ltd. This is an open access article under the CC BY license (<http://creativecommons.org/licenses/by/4.0/>).

cooking and/or extraction methods. It seems that dried ginger is superior to the fresh one (Mao et al., 2019a).

The other interesting property attributed to ginger and its derivatives is the anti-inflammatory one. The most relevant components of ginger involved in controlling inflammation are shogaols (Shim et al., 2011), gingerols (Ho et al., 2013), and gingerdione (Li et al., 2012). Inflammation is a protective defence response to deleterious stimuli, such as infection, or tissue injury. Macrophages are essential to host immune defences against pathogens by inducing a cascade of signalling events to rescue the immune homeostasis. Within the molecules modulating macrophages functions, the Toll-like receptors (TLRs) constitute a key family of pattern recognition receptors orchestrating inflammatory responses through a series of well-characterized downstream cascades (Qian & Cao, 2013). For example, the binding of the lipopolysaccharide (LPS), a toxin outside the membrane of gram-negative bacteria, to TLR4 generates an immune response. The activation of TLR4, in turn, induces adaptor proteins (i.e., MyD88), triggering signalling cascades (i.e., activating NF- κ B and MAPKs) that culminate in the production of pro-inflammatory cytokines (Kawai & Akira, 2007).

For such reasons, macrophage cell lines are typically used in inflammation studies. Particularly, RAW264.7 macrophages are mediator cells involved in inflammatory and infectious events, directly via phagocytosis of pathogens and indirectly via secretion of pro-inflammatory cytokines. They are also considered an important model to study the immunomodulatory response to the action of many molecules (Yang & Ming, 2014). Plasticity and flexibility are key features of macrophages, which are manifested by their aptitude to undergo alternative phenotypes, known as “polarization”, induced by different stimuli. Two cellular subtypes, denominated M1 or M2, are produced by polarization, although a plethora of intermediate phenotypes exists. They have opposite characteristics and functions, where M1 (classical or “pro-inflammatory” phenotype) that promotes inflammation in tissues, whereas M2-like (alternative or “anti-inflammatory” phenotype) has the ability to wound healing and dampening of inflammation (Martinez & Gordon, 2014).

Despite the large number of investigations on the subject, the data obtained from *in vitro/in vivo* experimental and clinical studies on the potential protective and/or therapeutic role of ginger extracts are clinically heterogeneous, far from clarifying the underlying mechanisms and not conclusive, thus decreasing the confidence in the available results.

This study was designed to obtain a new total ginger extract (GE) by a simplified ethanol and freeze-drying method, which was chemically characterised and whose efficacy as an anti-inflammatory and/or antioxidant was investigated at molecular level. We analysed the differential expression of some genes involved in the TLR4 signalling pathway, as well as in the promotion of macrophages polarization, in RAW264.7 murine macrophage cells pre-treated with GE, or with the commercial [6]-gingerol, and stimulated by LPS. Overall results showed that GE reduce the LPS-induced inflammatory/oxidative responses and promote polarization of macrophages.

2. Materials and methods

2.1. Ginger extraction

The ginger extraction protocol was modified from Ok and Jeon (Ok & Jeong, 2012). Fresh ginger rhizome, purchased from a grocery store in Palermo, was sliced into small pieces, frozen and stored at -20°C . After thawing, 96% ethanol (EtOH) was added to ginger slices in a 1:30 solid/liquid ratio and left under stirring at 24°C for 72 h. The extract was subjected to freeze-drying in a cold freeze dryer (Scanvac coolsafe, Labogene, Lyngø, Denmark) and finally frozen at -20°C . The lyophilized extract was suspended in EtOH, filtered with a $0.22\ \mu\text{m}$ nylon filter, aliquoted in Eppendorf tubes and freeze-dried again. Each aliquot containing 20 mg of freeze-dried ginger was suspended in EtOH at the

appropriate concentrations for the subsequent analyses, for a maximum of four weeks.

2.2. Total phenolic content by Folin-Ciocalteu method

Total content of phenolic compounds of GE was determined by Folin-Ciocalteu assay in agreement with Gutfinger (Gutfinger, 1981) with slight modifications. Freeze-dried aliquot (20 mg) of GE was dissolved in 2 ml EtOH. Then, 0.2 ml were diluted with water up to 5 ml and 0.5 ml Folin-Ciocalteu reagent were added. After 3 min, 1 ml of sodium carbonate solution (20%, w/v) was added to the reaction mixture, which was finally diluted to 10 ml volume with water. The absorbance of mixtures was measured after 2 h, in the dark, at 765 nm wavelength against a reagent blank. Gallic acid was used as standard for preparing the calibration curve in EtOH ranging 12.5–200 $\mu\text{g}/\text{ml}$. The total polyphenol content was expressed as mg of acid gallic equivalents (GAE) per gram of dry extract (DE).

2.3. Oxygen radical absorbance capacity (ORAC) assay

The ORAC assay was performed according to Ninfali (Ninfali et al., 2002) with slight modifications. The reaction mixture was prepared in a 96-well black microplate as follows: 160 μl of 0.04 μM Fluorescein in 0.075 M Na–K phosphate buffer pH 7.0, 20 μl of appropriately diluted sample or 20 μl of 100 μM Trolox, the latter being a synthetic vitamin E analogue with antioxidant activity used as reference standard. Each mixture was kept 10 min at 37°C in the dark, and the reaction was started with the addition of 20 μl of 40 mM 2,2'-azobis(2-methylpropionamide) dihydrochloride (AAPH). The fluorescence intensity decay was measured at 37°C every 1 min at 485 nm excitation and 538 nm emission wavelengths respectively, using a Fluoroskan Ascent F2 Microplate (Thermo Fisher Scientific, Massachusetts, USA). The ORAC value refers to the area under the curve (AUC) of Fluorescein decay in the presence of GE or Trolox, subtracted of the blank area. The activity of the sample was expressed as μM of Trolox Equivalents (TE)/g of Dry Extract (DE), with the following equation:

$$\text{ORAC value } (\mu\text{mol TEg}^{-1}) = k \cdot a \cdot h \left[\frac{(S_{\text{sample}} - S_{\text{blank}})}{(S_{\text{Trolox}} - S_{\text{blank}})} \right] \quad (1)$$

where k is the final dilution of the extract; a is the ratio between the volume (litres) of GE and grams of dried extract; h is the final concentration of Trolox expressed as $\mu\text{mol}/\text{l}$; S is the area under the curve of fluorescein in the presence of sample, Trolox, or buffer solution.

2.4. High performance liquid chromatography (HPLC) analysis

Identification and quantification of [6]-gingerol in GE sample were obtained by HPLC investigations by comparison with [6]-gingerol standard. Chromatographic measurements were performed with a HPLC system (LC-2010 AT Prominence, Shimadzu, Kyoto, Japan) equipped with an UV/Vis photodiode array detector (SPD-M20A), an on-line degasser system (DGU 20A5), and 20 μL sample loop. A Supelco Discovery C18 ($4 \times 250\ \text{mm}$, $5\ \mu\text{m}$ Sigma-Aldrich, USA) column,

Table 1

The HPLC gradient elution program. Solvent A, 0.2% H_3PO_4 (V/V); solvent B, ethanol; solvent C, acetonitrile.

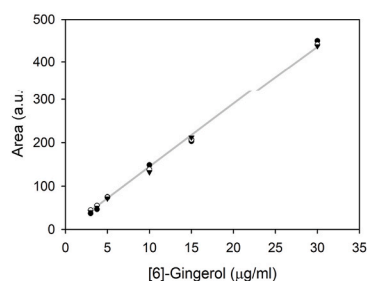
Time (min)	Solvent A%	Solvent B%	Solvent C %
0	96	2	2
40	50	25	25
45	40	30	30
60	0	50	50
70	0	50	50
72	40	30	30
82	96	2	2

maintained at 25 °C, was employed. The three solvents used as mobile phase and the programmed elution gradient used are reported in Table 1.

The UV-vis spectrum from 200 to 600 nm was acquired and 280 nm wavelengths were extracted to create the chromatographic profiles of interest. Calibration curve of [6]-gingerol was obtained by injecting 20 µl of increasing concentrations (3.0– 3.6 – 5.0– 6.0 – 15.0– 30.0 µg/ml) of standard compound ([6]-gingerol, G1046, Sigma-Aldrich) solubilized in EtOH. The resulting area of each peak, estimated at wavelength 280 nm, was plotted (squares) as function of concentration as shown in the graph below. The slope obtained from the linear fit

$$y = mx \quad (2)$$

(y is the area of peaks at different concentrations; x is the relative concentration of injected standard sample; and m is the angular coefficient of the linear fit) was used to calculate the concentration of [6]-gingerol in GE sample. All injections were performed in triplicate.



2.5. Treatments of RAW264.7 cells with GE and [6]-gingerol

Cell viability and qPCR analyses were performed using RAW264.7 murine macrophage cells and the procedure of treatments with GE or [6]-gingerol was the same for all these experiments. The cell line was obtained from the American Type Culture Collection (ATCC, Rockville, MD, USA) and maintained in culture using Dulbecco's modified Eagle's medium (DMEM, Gibco, Grand Island, NY, USA) supplemented with 10% FCS (DMEM/FCS), 100 U/ml of penicillin, 100 µg/ml of streptomycin (Gibco). Cells were grown in a humidified incubator at 37 °C and 5% CO₂.

RAW264.7 were seeded in multiwell plates in DMEM/FCS, at different densities depending on the size of the wells and treated with GE or [6]-gingerol at different concentrations (see each specific paragraph) for 2 h at 37 °C, followed by the addition of 0.1 µg/ml LPS. After incubation for 24 h at 37 °C, cells were harvested for each analysis.

2.6. Glutathione/oxidized glutathione (GSH) antioxidant assay

GSH/GSSG ratio quantification was conducted using the GSH/GSSG-Glo™ Assay (Promega, Madison, WI, USA). RAW264.7 were plated at a concentration of 2×10^4 cells/well in 96-well white plates in DMEM/FCS. 24 h later, the cells were pre-treated with 100 µg/ml GE for 2 h, and with or without 0.1 µg/ml LPS (positive control) for 24 h. After treatment, media was removed, and the assay was conducted according to the manufacturer's instructions. Luminescence was measured using the GloMax Discover System (GM3000; Promega). GSH/GSSG ratio was calculated using the following equation: $GSH/GSSG = [Total\ GSH - (2 \times X\ GSSG)]/GSSG$.

2.7. Cell viability test

Cell viability of RAW264.7 after 24h-treatments with GE (50, 75, 100, 200 µg/ml), [6]-gingerol (42.5, 85, 170 µM) or LPS (0.1 µg/ml) was evaluated by the MTS assay, using the CellTiter 96 Aqueous One

Solution Cell Proliferation Assay Kit (Promega), a colorimetric method for determining the number of viable cells in proliferation, according to the manufacturer's procedure. RAW264.7 were seeded at a density of 2×10^4 cells/well in 100 µl DMEM/FCS in 96-well plates and treated as previously described ("Treatments of RAW264.7 cells with GE and [6]-gingerol" section). Untreated cells (-) or cells treated with LPS alone (LPS) were used as controls. Kit reagent solution (20 µl) was added to each well and plates were incubated for 3 h at 37 °C. The absorbance was measured at 490 nm by GloMax Discover System (Promega). The results of cell viability are expressed as percentage.

2.8. RNA extraction and cDNA synthesis from RAW264.7 treated with GE, [6]-gingerol and LPS

For the gene expression analyses, cells were seeded in 12-well plates at 2×10^5 cells/ml and treated as previously described. After treatments, cells were washed with PBS to eliminate any dead cells and plates were kept dry at -20 °C. RNA was extracted from the following samples: untreated cells (Control, C), cells treated with 50 and 100 µg/ml GE (GE50 and GE100 respectively), LPS (LPS), GE and LPS (GE + LPS) co-treated cells, as well as 170 µM [6]-gingerol ([6]-ging) treated cells, [6]-gingerol and LPS ([6]-ging + LPS) co-treated cells, using the GenElute Mammalian Total RNA Miniprep Kit (RTN70; Sigma-Aldrich), according to the manufacturer's instructions. RNA was quantified using a bio-photometer D30 (Eppendorf, Hamburg, Germany, Europe). Total RNA (1 µg) was reverse transcribed with the High-Capacity cDNA Reverse Transcription Kit according to the manufacturer's instructions (4368814; Applied Biosystems, Life Technologies, Carlsbad, CA, USA).

2.9. Real-time quantitative polymerase chain reaction (qPCR)

Quantification of gene expression was done using a real-time PCR (StepOnePlus, Applied Biosystems), according to the manufacturer's manual. A comparative threshold cycle method with SYBR Green master mix was used. Relative quantification was performed by the $\Delta\Delta CT$ method with the formula $2^{-\Delta\Delta CT}$. The qPCR was carried out as follows: 1 cycle denaturing 95 °C for 10 min for DNA polymerase activation, 38 cycles, melting at 95 °C for 15 s and annealing/extension at 60 °C for 60 s. The amplification reaction was performed with the quantitect specific primers (Qiagen, Venlo, Netherlands, Europe) for mouse genes, described in Table S1. GAPDH was used as endogenous gene, to normalize data from other genes. Custom primers were validated by sequencing of the obtained amplicon. Primers' specificity was confirmed by the "melting curve", during PCR reaction.

2.10. Statistical analysis

The statistical significance of the results was assessed using Student's t-test on Microsoft Excel, setting a two-tailed distribution, with significance at $p < 0.05, 0.01, 0.001$, and was done for qPCR values obtained from at least three independent experiments.

2.11. STRING analysis

The predicted protein-protein interactions among all the proteins encoded by the genes analysed in this study was obtained from STRING database (<http://string-db.org/>, last accessed March 13, 2023) (Szklarczyk et al., 2023). In detail, the research has been performed selecting *Mus musculus* as input organism and "multiple proteins" mode. Proteins and corresponding UniProt ID were reported in Table S1. The network analysis was performed taking into consideration the following "evidence channels", textmining, known (databases, experiments) and predicted (gene neighbourhood, co-occurrence) interactions, co-expression. The interaction score was set at "low confidence" (0.150) to expand the number of predicted interactions.

3. Results

3.1. Extraction of GE and characterization by total phenolic content and HPLC analyses

The EtOH extraction of ginger rhizome was based on the protocol of Ok and Jeon (Ok & Jeong, 2012) with some modifications, mainly concerning the freeze-drying and temperature extraction cycles.

The phenolic compounds of ginger have been related to many bioactivities, including the anti-inflammatory and antioxidant ones (Ali et al., 2018; Mustafa et al., 2019). We evaluated the total phenolic content (TPC) in samples of GE used in *in vitro* cell experiments by the Folin-Ciocalteu spectrophotometric method. TPC value is shown in Table 2.

To investigate the antioxidant ability of the new GE, we used the ORAC assay, a fast method to measure the capacity of a pure compound or complex mixtures to scavenge the free radicals (Dávalos et al., 2004). ORAC assay is based on the ability of an antioxidant to prevent the fluorescein oxidation caused by a free radical generator AAPH, thus maintaining its intensity. Fig. 1 shows the fluorescence decay curves in the presence of Trolox, a reference standard, GE and the related blanks (PBS, EtOH). The fluorescence signal stabilized in the presence of GE indicated an effective protection of fluorescein against oxidation. After calculating the net area of fluorescein decay under each curve (AUC) and applying the equation reported in Materials and methods Section, the high ORAC value obtained denoted a strong antioxidant activity of the GE sample (Table 2).

Finally, we focused our chemical characterization of GE on [6]-gingerol identification and quantification. Fig. 2A shows the chromatographic profile of GE at 280 nm wavelength. The signal shows a sequence of peaks including a dominant one that was identified as [6]-gingerol by comparison of retention time and UV spectrum of the dominant peak of GE (Fig. 2A and inset) with ones of [6]-gingerol standard (Fig. 2B and inset). The amount of [6]-gingerol in GE was estimated by a calibration curve of the standard and it was determined in mg per gram of dry extract (DE) (Table 2).

3.2. Effects of GE on viability and morphology of RAW264.7

Before studying the anti-inflammatory and immunomodulatory effects of GE, its working concentrations were determined by evaluating cell viability and impact on cell morphology. Cell viability was evaluated in RAW264.7 treated with different concentrations of GE (50, 75, 100, 200 µg/ml) or 0.1 µg/ml LPS (which mimics a bacterial infection) for 24 h and analysed using MTS assay (see the experimental scheme in Fig. 3A). As shown in Fig. 3B, cells were viable at all the GE concentrations used. On this result, we decided to use the 50 and 100 µg/ml concentrations of GE in the following experiments.

GE did not change the morphology of the RAW264.7 population, which normally include at least three different shapes, mainly bipolar spindle-shaped and round, as well as flattened with short cytoplasmic projections, representing diverse aspects of the cell behaviour, i.e., migration, cell division and stationary state (Fig. 3C). Furthermore, it appeared that GE was able to slightly reduce the degree of altered morphologies obtained by LPS treatment. LPS-treated cells lost their normal shape showing extremely irregular edges and highly granular cytoplasm with several vacuoles, while the GE pre-treatment partially

Table 2

Total phenolic content (TPC), Oxygen Radical Absorbance Capacity (ORAC) and [6]-gingerol content values of the ethanolic extract of ginger (GE).

Sample	TPC (mg GAE/g DE)	ORAC (µmol TE/g DE)	[6]-gingerol (mg/g DE)
GE	4.4 ± 0.16	227.79 ± 10.4	3.2 ± 0.02

Values are mean from 3 different experiments ± SD.

GAE, acid gallic equivalents; DE, dry extract; TE, Trolox Equivalents.

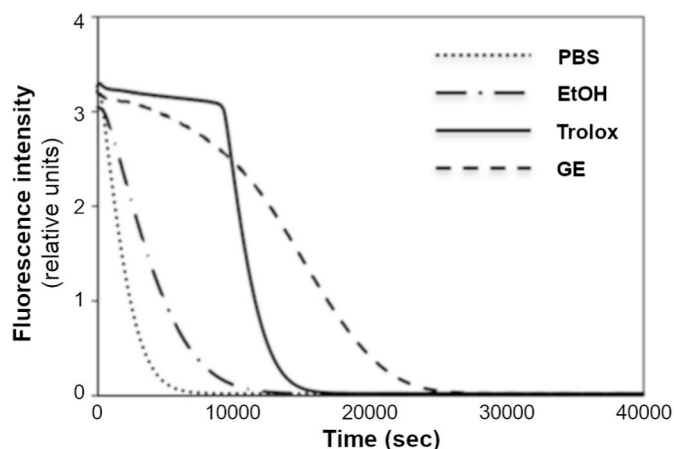


Fig. 1. Antioxidant ability and total phenolic content of GE. Fluorescence decay curves obtained by oxygen radical absorbance capacity (ORAC) assay. GE curve is shown as dashed line and the curve of Trolox, used as standard reference, as continuous line. Blank (PBS) and sample blank (EtOH) curves are shown as dot and dot-dashed lines, respectively.

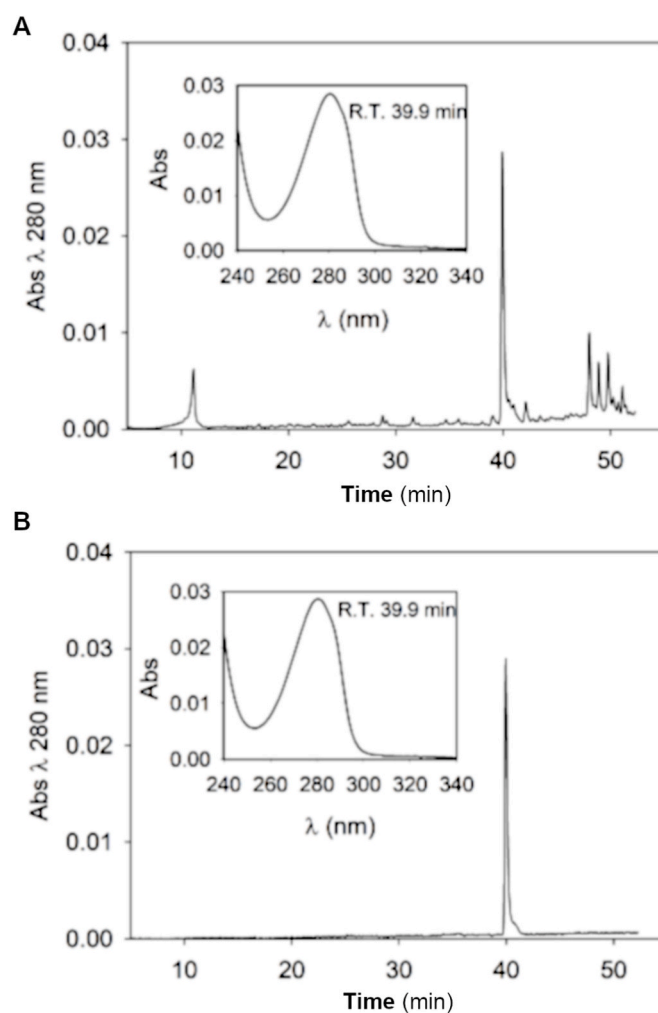


Fig. 2. HPLC analysis of GE. Chromatograms profiles registered at 280 nm wavelength for GE (A) and for [6]-gingerol standard (B). The insets show the spectrum acquired at the specified retention time.

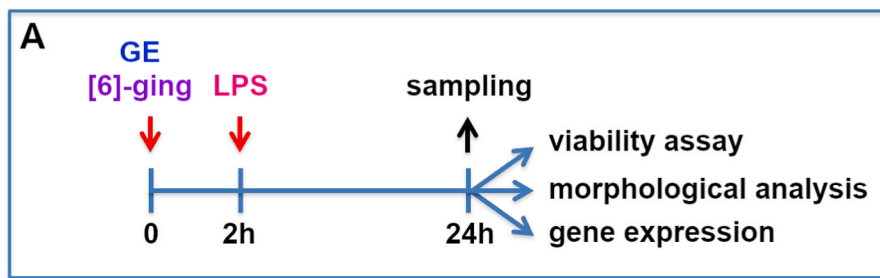
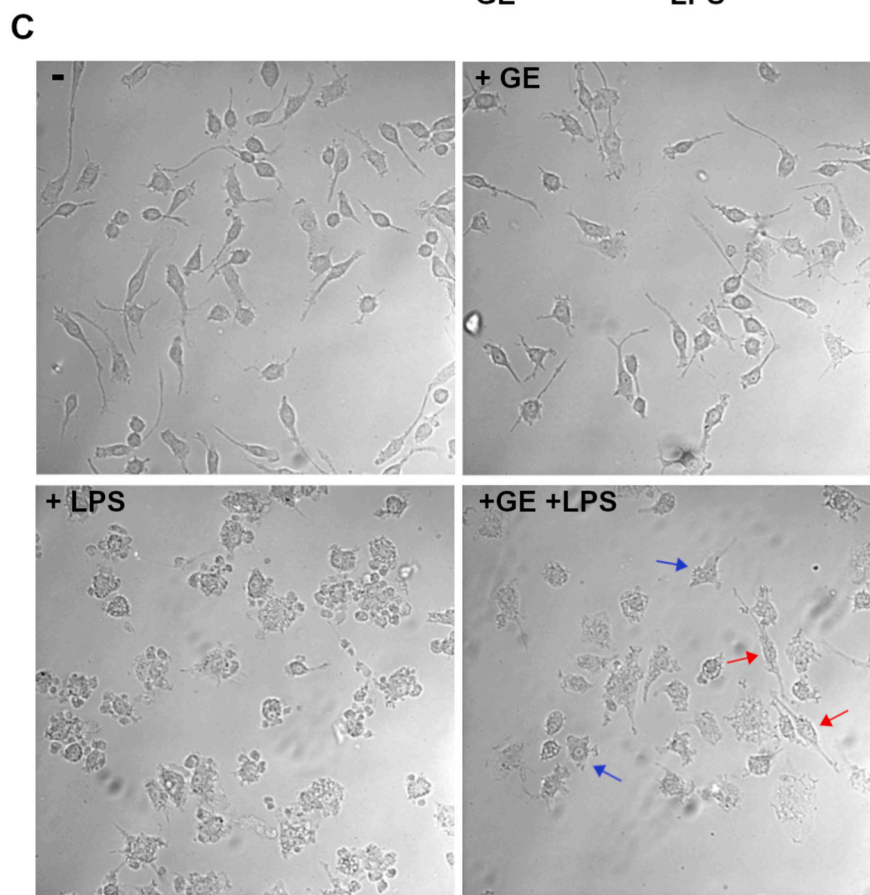
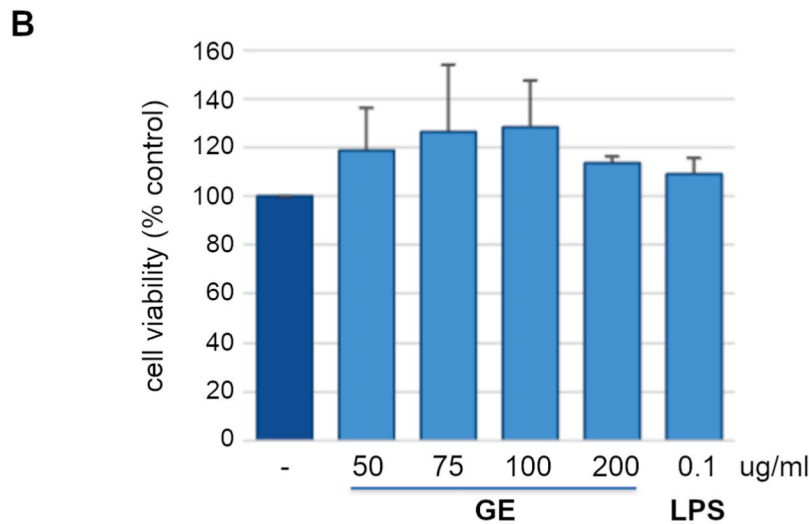


Fig. 3. Effects of GE on RAW264.7 cells viability and morphology. A) Schematic drawing depicting the experimental procedure. RAW264.7 cells were treated with different concentrations of GE or [6]-gingerol for 2 h at 37 °C, followed by the addition of 0.1 µg/ml LPS. After incubation for 24 h at 37 °C, cells were harvested for each different analysis (sampling), i.e., viability assay, morphological and gene expression analyses. B) MTS cell viability test on RAW264.7 cells untreated (-) or treated with 50, 75, 100, 200 µg/ml GE or 0.1 µg/ml LPS. The results of cell viability are expressed as percentage of the untreated control cells ± SD. C) Morphology of untreated (-) cells, or 100 µg/ml GE (GE), 0.1 µg/ml LPS (LPS) or 100 µg/ml GE + 0.1 µg/ml LPS (+GE + LPS) treated cells, observed 24 h after treatments. Red arrows point to bipolar spindle-shaped cells, blue arrows point to flattened cells. (For interpretation of the references to colour in this figure legend, the reader is referred to the Web version of this article.)



retained the cell shapes (red arrows indicating some bipolar spindle-shaped cells and blue arrows indicating flattened cells), although some cells with granular cytoplasm and some vacuoles were still visible (Fig. 3C).

To confirm the antioxidant property of GE at the cellular level, we used the glutathione (GSH) assay. GSH is the most abundant endogenous antioxidant in the cell and works in tandem with NADPH to neutralize ROS in cells. The ratio of GSH to its disulphide form GSSG is widely used as an indicator of the redox state of the GSH pool, as the balance of reduced GSH and oxidized GSSG may reflect oxidative stress and changes in redox signalling and control (Jones, 2002). The GSH assay was performed on RAW264.7 treated with 100 $\mu\text{g}/\text{ml}$ GE (GE100), LPS and GE100 + LPS. GE100 significantly increased the GSH/GSSG ratio, and rescued the reduction caused by the LPS treatment, confirming its antioxidant activity (Fig. 4).

3.3. Effects of commercial [6]-gingerol on viability and morphology of RAW264.7

After having ascertained by HPLC analysis that the GE contained primarily [6]-gingerol, we determined working concentrations of commercial [6]-gingerol by evaluating cell viability and impact on cell morphology, before performing investigations at molecular level. Cell viability was evaluated in cells treated with different concentrations of [6]-gingerol (42.5, 85 and 170 μM) for 24 h and analysed by MTS assay (Fig. 5A). The cells were viable at all the [6]-gingerol concentrations tested, thus indicating that they were not toxic for cells.

The analysis of the cells at morphological level showed that, even at the highest concentration tested (170 μM), [6]-gingerol did not have deleterious effects on cells, which indeed appeared like controls (Fig. 5B).

3.4. Molecular effects of GE and [6]-gingerol in cells exposed to LPS

To study the potential role exerted by our GE in the cellular response against an LPS insult, we analysed the mRNA levels of distinct categories of genes i.e., immune signalling (TLR4, MyD88, Jun, Rel-A), pro/anti-inflammatory cytokines (IL-1 α , IL-6, TNF- α , IL-10), hallmarks of macrophage polarization (Light1/Tnfsf14, Mif), as well as pro-/antioxidant molecules (iNOS, HO-1, Arg-1) and an endoplasmic reticulum (ER)

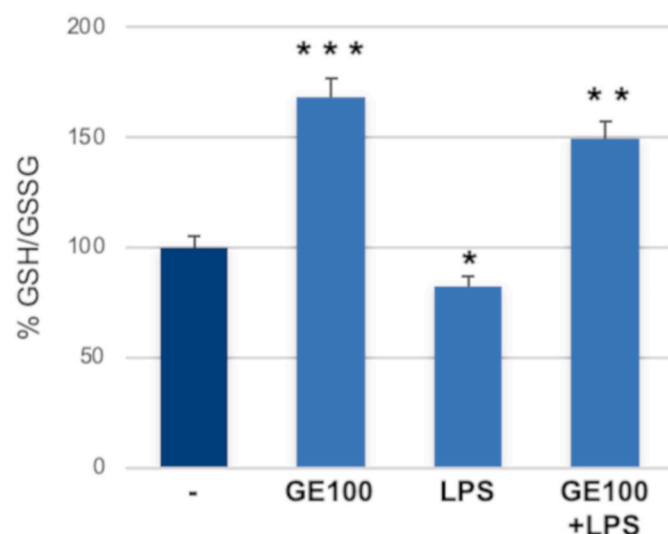


Fig. 4. Antioxidant property of GE at cellular level. GSH assay was performed on RAW264.7 cells untreated (–) or treated with 100 $\mu\text{g}/\text{ml}$ GE (GE100), LPS and GE100 + LPS. The GSH/GSSG ratio was expressed as percentage referred to untreated cells, set as 100% in the histogram, $\pm\text{SD}$. *** ($p < 0.001$), ** ($p < 0.01$), * ($p < 0.05$).

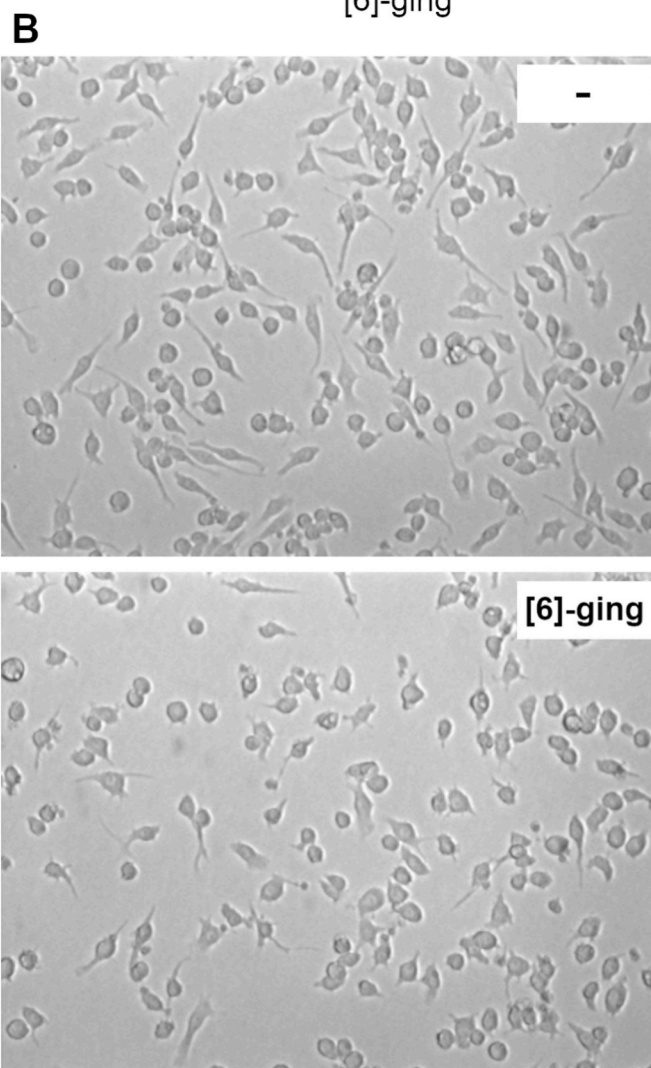
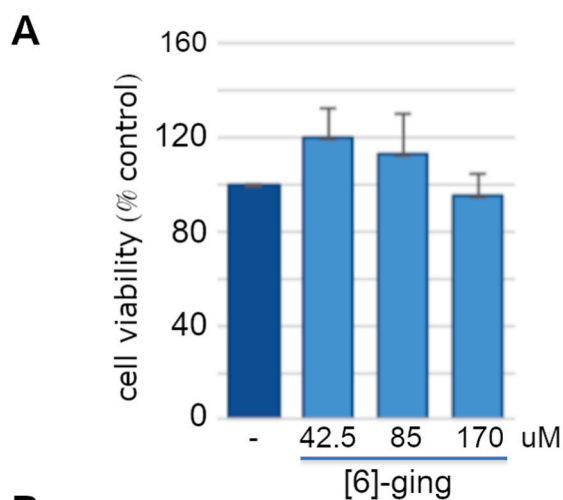


Fig. 5. Effects of [6]-gingerol on RAW264.7 cells viability and morphology. A) MTS cell viability test on RAW 264.7 cells untreated (–) or treated with 42.5, 85, 170 μM [6]-gingerol for 24 h at 37 $^{\circ}\text{C}$. The results of cell viability are expressed as percentage of the untreated control cells $\pm\text{SD}$. B) Morphological analysis of RAW264.7 cells untreated (–) or treated with 170 μM [6]-gingerol, monitored 24 h after treatment.

stress gene (TRIB3). QPCR experiments were performed on RAW264.7 treated with LPS for 24 h, after a 2 h pre-treatment with 50 or 100 µg/ml GE (GE50/100 + LPS), using untreated cells as controls (C). To understand the following molecular analyses, it is important to point out that the substantial effects of GE and [6]-gingerol on gene expression in RAW264.7 were detected by the following normalization procedure: changes of the mRNA levels in cells treated with GE, [6]-ging and LPS were normalized against untreated control cells (statistical significance shown by (+) signs in Figs. 6–8), whereas the values of GE/[6]-ging +

LPS treated cells were normalized against those of LPS-treated cells (asterisks in Figs. 6–8).

Within the immune signalling category, the pre-treatment with GE decreased the LPS-induced expression of TLR4 and MyD88 genes in comparison with LPS control cells (Fig. 6). This effect was dependent upon the GE concentration, with the 100 µg/ml dose being the most effective and significant for both genes, i.e., 1.38 vs. 0.55-fold change for TLR4 and 1.53 vs. 0.76-fold change for MyD88 (Fig. 6).

The expression of Jun, a transcription factor of the AP-1 complex,

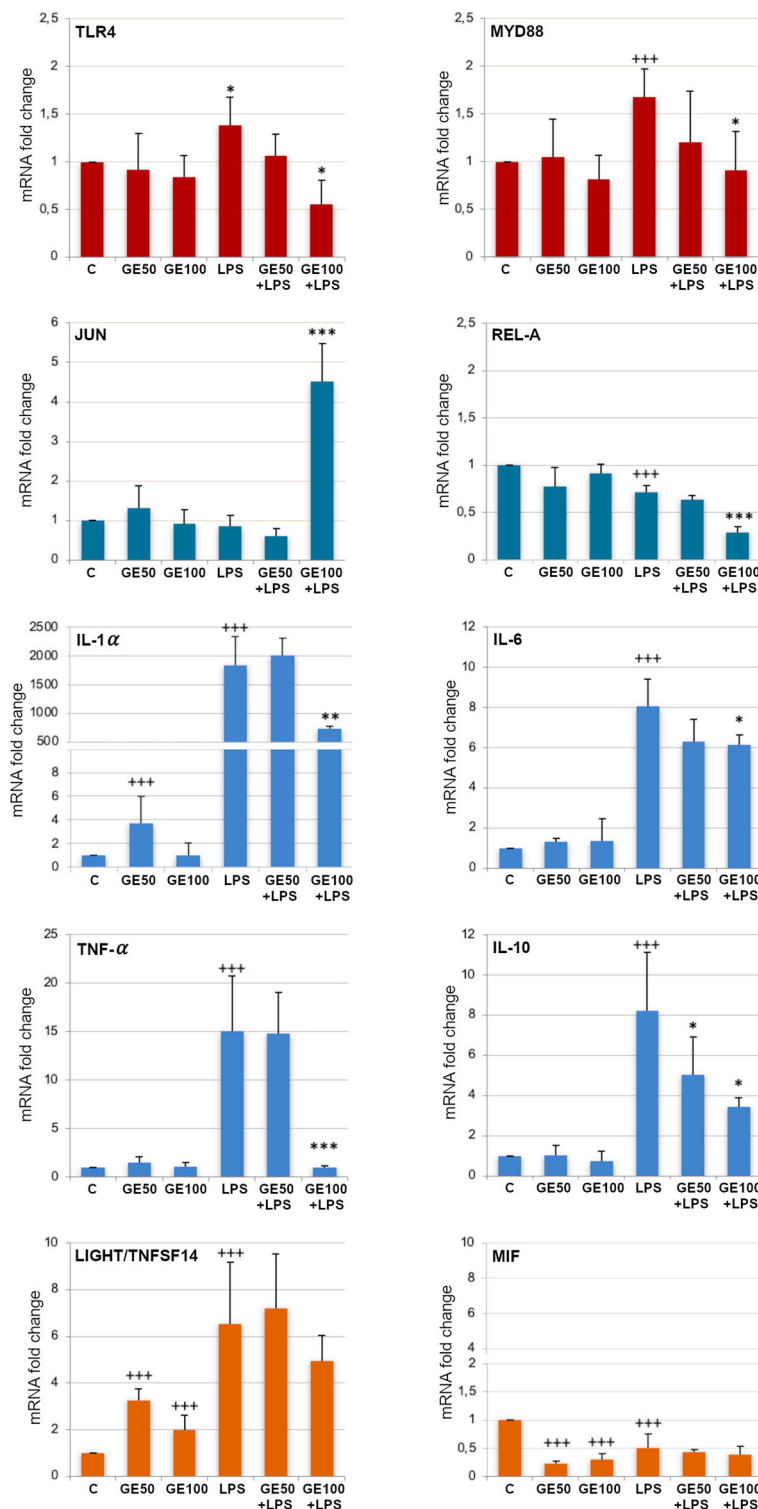


Fig. 6. Molecular effects of GE on RAW264.7 cells. The quantitative analysis of gene expression was performed by qPCR. Cells were treated with GE, at the concentrations of 50 (GE50) and 100 (GE100) µg/ml, 0.1 µg/ml LPS (LPS), or pre-treated with 50/100 µg/ml GE for 2 h followed by LPS addition (GE50 + LPS and GE100 + LPS respectively), for 24 h. Relative mRNA levels are expressed as fold changes compared to control sample (C), at which was assigned an arbitrary value of 1 in the histogram. Each bar represents the mean of three independent experiments. The GAPDH gene was used as the endogenous reference gene for normalization. The plus (+) indicates statistically significant difference between GE50, GE100 or LPS-treated cells and control (C) cells, +++ (p < 0.001), ++ (p < 0.01), + (p < 0.05). The asterisks indicate statistically significant differences between GE50 + LPS, GE100 + LPS and LPS treated cells, *** (p < 0.001), ** (p < 0.01), * (p < 0.05).

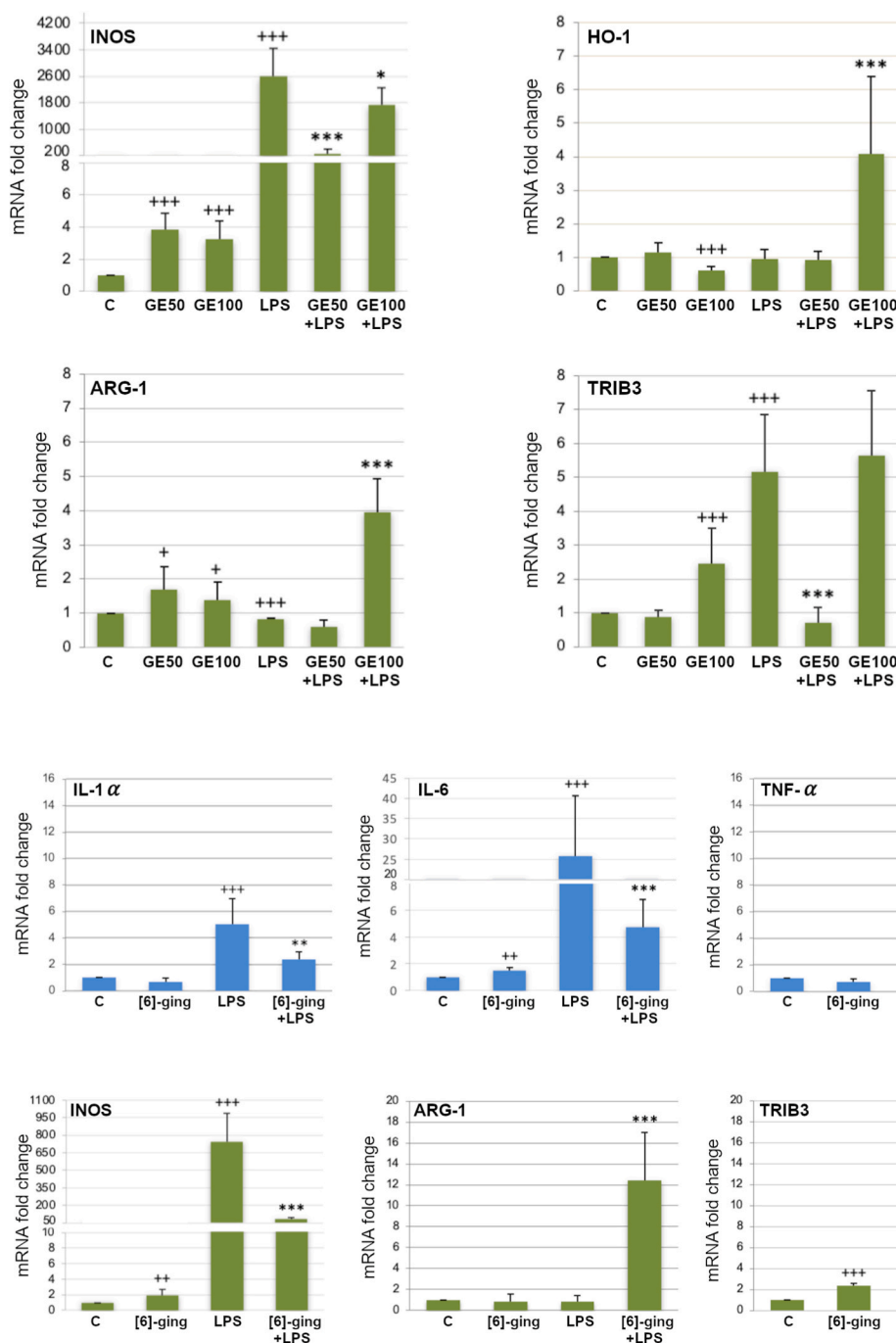


Fig. 7. Molecular effects of GE on RAW264.7 cells. The quantitative analysis of gene expression was performed by qPCR. Cells were treated with GE, at the concentrations of 50 (GE50) and 100 (GE100) $\mu\text{g}/\text{ml}$, 0.1 $\mu\text{g}/\text{ml}$ LPS (LPS), or pre-treated with 50/100 $\mu\text{g}/\text{ml}$ GE for 2 h followed by LPS addition (GE50 + LPS and GE100 + LPS respectively), for 24 h. Relative mRNA levels are expressed as fold changes compared to control sample (C), at which was assigned an arbitrary value of 1 in the histogram. Each bar represents the mean of three independent experiments. The GAPDH gene was used as the endogenous reference gene for normalization. The plus (+) indicates statistically significant difference between GE50, GE100 or LPS-treated cells and control (C) cells, +++ ($p < 0.001$), ++ ($p < 0.01$), + ($p < 0.05$). The asterisks indicate statistically significant differences between GE50 + LPS, GE100 + LPS and LPS treated cells, *** ($p < 0.001$), ** ($p < 0.01$), * ($p < 0.05$).

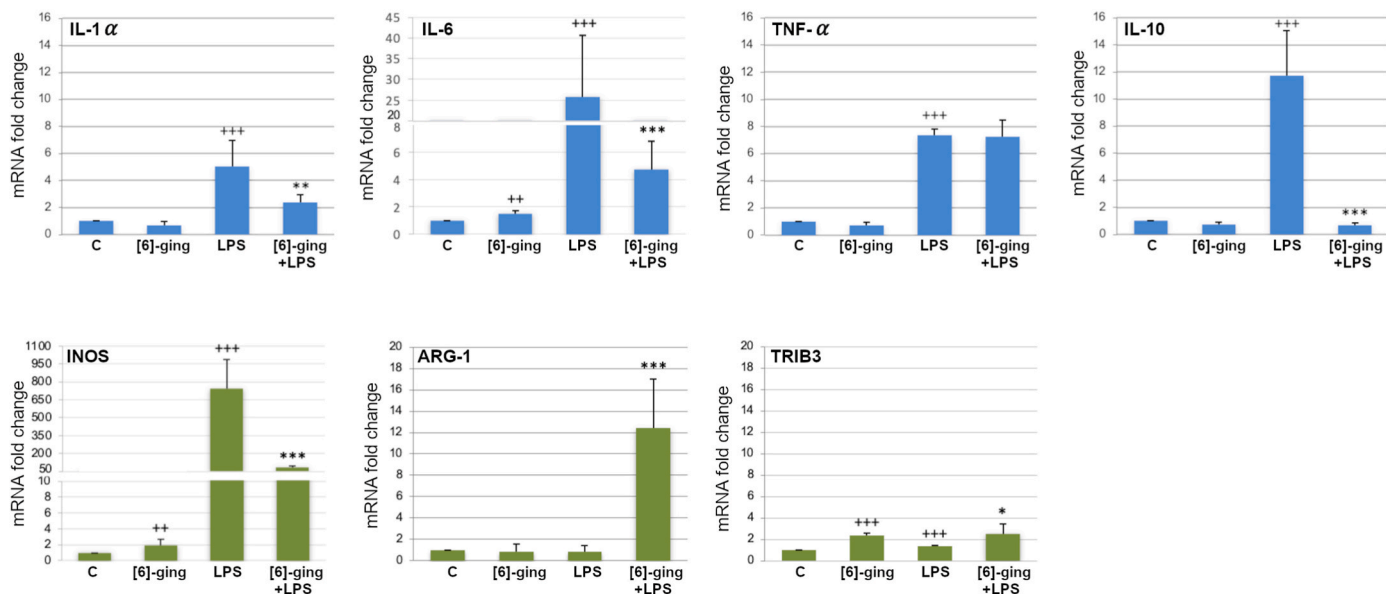


Fig. 8. Molecular effects of [6]-gingerol on RAW264.7 cells. The quantitative analysis of gene expression was performed by qPCR. Cells were treated with 170 μM [6]-gingerol ([6]-ging), 0.1 $\mu\text{g}/\text{ml}$ LPS (LPS), or pre-treated with 170 μM [6]-gingerol for 2 h followed by LPS addition ([6]-ging + LPS). Relative mRNA levels are expressed as fold changes compared to control sample (C), at which was assigned an arbitrary value of 1 in the histograms. Each bar represents the mean of three independent experiments. The GAPDH gene was used as the endogenous reference gene for normalization. The plus (+) indicates statistically significant difference between [6]-ging or LPS treated cells and control (C) cells, +++ ($p < 0.001$), ++ ($p < 0.01$), + ($p < 0.05$). The asterisks indicate statistically significant differences between [6]-ging + LPS and LPS treated cells, *** ($p < 0.001$), ** ($p < 0.01$), * ($p < 0.05$).

was not affected by GE treatment alone and in LPS-treated cells (Fig. 6). Interestingly, the Jun mRNA levels increased markedly and significantly in GE100 + LPS cells, i.e., about 4.5-fold compared to LPS-treated cells.

Rel-A is a subunit of NF- κB , a transcription factor playing a role in inflammatory response. In our qPCR experiments, the levels of Rel-A mRNAs slightly and significantly decreased in LPS-treated cells, compared to control cells, and even more in GE100 + LPS cells (0.29-fold decrease), compared to LPS-treated cells (Fig. 6).

As expected, RAW264.7 macrophages showed severe inflammatory

responses after LPS treatment, manifested by the significant increased levels of IL-1 α , IL-6, TNF- α and IL-10 mRNAs, with more than 8 up to 1833 orders of magnitude compared with controls (Fig. 6). These inductions were more or less efficiently reversed by the pre-treatment with GE, especially at the maximum dose of 100 $\mu\text{g}/\text{ml}$, which significantly reduced mRNAs levels of all these genes, even though by different orders of magnitude. The levels of IL-10 mRNA were reduced in a dose-dependent manner by GE50/100 pre-treatments, compared to LPS control.

The mRNA levels of Light/Tnfsf14, a member of TNF ligand family, were increased by all the treatments performed, i.e., both doses of GE (3.2- and 2-fold, respectively), LPS alone (6.5-fold), and GE50/100 + LPS that maintained the LPS-induced high expression (7.2- and 4.9-fold, respectively) (Fig. 6). Contrarily, the mRNA levels of macrophage migration inhibitory factor (MIF), a regulator of innate immunity and inflammation, decreased significantly with all treatments, i.e., with GE50/100 and LPS alone (changes from 0.5- to 0.2-fold), while no effect was detected comparing GE50/100 + LPS treated cells with those treated with LPS (Fig. 6).

Within the group of pro-/antioxidant molecules, iNOS mRNA levels increased significantly in LPS-treated cells (2600-fold) compared to control cells, while they were severely reduced by pre-treatment with 50 µg/ml GE (266-fold), and less effectively by 100 µg/ml GE (1737-fold) (Fig. 7). There was also an interesting increase of iNOS mRNA levels when GE was used alone, both doses, compared with the control (3.8- and 3.2-fold respectively).

LPS treatment essentially did not affect HO-1 mRNA levels and slightly decreased those of Arg-1. In accordance with antioxidant properties of GE, they were both highly increased (4-fold) by the GE100-pretreatment. A slight increase of Arg-1 mRNAs levels was also observed when GE was used alone (Fig. 7).

The mRNA levels of Tribbles Pseudokinase 3 (TRIB3), a marker of ER stress, were increased by treatments with 100 µg/ml GE (2.4-fold) and LPS (5.1-fold), while they were severely reduced by GE50-pretreatment (GE50 + LPS) compared to LPS-treated cells (Fig. 7). Contrarily, GE100-pretreatment (GE100 + LPS) was not effective in reducing LPS-induced TRIB3 mRNA levels.

A partial gene expression analysis has also been performed on cells pre-treated with commercial [6]-gingerol (170 µM), the major component of GE, studying its effect on the cellular response evoked by the LPS stimulus, to identify any similarities with respect to GE pre-treatments. Similarly, to what was observed for GE, the pre-treatment with [6]-gingerol ([6]-ging + LPS) reduced the LPS-induced mRNA levels of the investigated cytokines, IL-1α, IL-6, and IL-10 (Fig. 8). Conversely, [6]-gingerol pre-treatment failed to reduce the LPS-induced TNF-α mRNA levels.

A trend like GE treatment was also observed for iNOS and Arg-1 mRNAs. [6]-gingerol pre-treatment remarkably reduced the LPS-induced levels of iNOS mRNA (745 vs. 79-fold change), whereas it highly increased the Arg-1 mRNA levels in LPS-treated cells (Fig. 8). A significant increase of iNOS mRNA levels (1.9-fold) was also observed when [6]-gingerol was used alone, compared with the control. The mRNA levels of TRIB3 were significantly increased by [6]-gingerol used alone (2.4-fold change) and when used as a pre-treatment before LPS (Fig. 8).

4. Discussion

Here, the potential anti-inflammatory and antioxidant properties of a new ginger extract (GE) were studied at chemical, cellular and molecular levels. We adapted the Ok and Jeong (Ok & Jeong, 2012) protocol to obtain a GE with prevalent [6]-gingerol content. Considering the thermal instability of gingerols, we did not use heat treatments, but applied an EtOH and freeze-drying extraction method. The GE was characterized by HPLC and antioxidant tests, and its anti-inflammatory/antioxidant effects were analysed on cells, extending the number of molecular marker analysed, compared to other studies (Liang et al., 2018). LPS-stimulated RAW264.7 murine macrophages were used as an *in vitro* inflammatory model to investigate the immunomodulatory effects of our GE and of commercial [6]-gingerol. All the results proved that GE has immunomodulatory, anti-inflammatory, and antioxidant effects after LPS stimulation, involving the differential expression of three categories of genes: immune signalling, anti-inflammatory cytokines, antioxidant, and hallmarks of macrophage polarization.

Various methods have been developed to extract bioactive compounds from ginger and several studies have also shown that different extraction methods can lead to variable concentrations of the components in the extract, which includes phenolic compounds, terpenes, polysaccharides, lipids, organic acids, and raw fibres (Mao et al., 2019a; Mustafa et al., 2019). Therefore, even the extent of the biological properties varies according to the percentages of the various compounds and in turn to the extraction method used (Mustafa et al., 2019). This is an important aspect to consider when comparing plant extracts obtained with different methods, as appropriate chemical/biological analyses are required before using their bioactive molecules. The extraction method used here, generated a GE containing [6]-gingerol, but with other unidentified components. It is likely that this GE may be different in its overall content and biological activities than others. However, the ethanol/freeze-drying extraction maintained the well-known characteristics of ginger, such as the total phenolic content and the antioxidant activity, as shown by the high ORAC value obtained, consistent with the literature data (Ninfali et al., 2002). The freeze-drying method is known to promote extraction processes causing cell wall rupture, leading to easier release of compounds into solvents, while retaining features closer to the characteristics of fresh plants (Hossain et al., 2010).

All the GE doses analysed here did not affect cell viability and had no effect on cell morphology. Moreover, the fact that GE somehow manages to partially prevent the morphological damage caused by LPS is interesting, as it suggests its potential protective action on the cells.

For molecular analyses, we have chosen genes with different functions, including those classically studied (pro-/anti-inflammatory, antioxidant), genes considered markers of macrophages polarization or involved in the ER stress response. We performed an *in silico* analysis, using the STRING database, to simulate known and/or possibly predicted connections among the proteins coded by the genes analysed here (Fig. 9). TLR4 and MyD88 showed the largest number of connections to all those proteins known to be involved in the TLR4 signalling pathway,

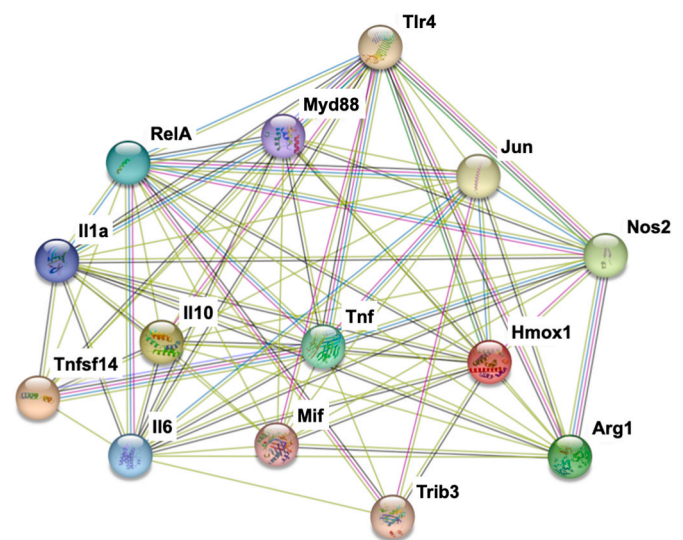


Fig. 9. Protein-protein network graphic. STRING analysis was used to construct the protein-protein network graphic to simulate predicted connections (displayed as coloured lines) among proteins (displayed as nodes) coded by the genes analysed here: Tlr4; Myd88; Rela (REL-A); Jun; Il1a (IL-1α); Il6 (IL-6); Il10 (IL-10); Tnf (Tnf-α); Nos2 (iNOS); Hmox1 (HO-1); Arg1 (ARG-1); Tnfsf14 (Light/TNFSF14); Mif; Trib3. *Mus musculus* was chosen as input organism. The network analysis was performed taking into consideration the following “evidence channels”, represented by the coloured lines in the graphic, i.e., text-mining (light green), databases (turquoise), experiments (fuchsia), gene neighbourhood (green), co-occurrence (blue), co-expression (black). (For interpretation of the references to colour in this figure legend, the reader is referred to the Web version of this article.)

including Rel-A, Jun and the cytokines. From this analysis, iNOS (Nos2), Arg-1, HO-1 (Hmox1) and TRIB3 also appeared to be involved in the TLR4 signalling pathway, as they were directly or indirectly (through Rel-A and Jun) connected with TLR4 (Fig. 9).

At molecular level, LPS has been confirmed to activate TLR4 signalling pathway in RAW264.7, inducing the expression of TLR4, MyD88, cytokines (IL-1 α , IL-6, TNF- α , IL-10), and the oxidant-inducible stress protein iNOS. In cell pre-treatment, our GE and commercial [6]-gingerol, appeared generally able of modulating the LPS-induced immune response and oxidative reactions, affecting the expression of the regulatory genes of these mechanisms, sometimes in a dose-dependent manner. Similar results were found using other natural compounds, i. e., morroniside, a glycoside compound of *Cornus officinalis* (Park et al., 2021) and xanthan gum, a microbial hetero-polysaccharide (Liu et al., 2017). Both compounds appear involved in the inhibition of LPS-induced inflammation and oxidative reactions in RAW264.7 by regulating TLR4 and HO-1 signalling pathways, suggesting a protective effect against inflammatory disorders.

TLR4 plays a key role in the identification of pathogens through the binding with polysaccharides present on their surfaces. Its activation induces MyD88, an adaptor protein, triggering signalling cascades, including activation of transcription factors (TFs), such as NF- κ B and AP-1, involved in the molecular mechanism of the immune/inflammatory responses. NF- κ B and Jun are among the early-response TFs, as they are present in cells as inactive proteins and their activation usually does not require new mRNA and protein synthesis, but only needs post-translational modifications. They are regulated by extracellular stimuli, including growth factors, cytokines, various forms of cellular stress (inflammation, oxidative stress, UV irradiation) (Karin et al., 1996; Kawai & Akira, 2010).

The NF- κ B family comprises five members, which pair each other to form different dimers with essential roles in the modulation of immune responses, as well as in the responses to bioactive compounds activities (De Sanctis et al., 2022; Mussbacher et al., 2023). NF- κ B activation is mainly regulated at protein level, through protein phosphorylation and translocation to the nucleus and partly at transcription level. The complex dynamics of NF- κ B signalling, including canonical/alternative signalling cascades, genetic networks, induction of feedback loops, have been extensively studied (Lawrence, 2009). The most abundant NF- κ B dimer contains Rel-A, generally functioning as transcriptional activator. The low levels of Rel-A mRNA observed after 24 h of LPS treatment are consistent with data previously reported (Sung et al., 2014). Authors showed that, 24 h after LPS-induction, Rel-A mRNA levels were as low as control levels in RAW264.7 cells, after a rapid increase within 5 h of LPS-treatment and decrease after 10 h. It will be interesting in future to examine what the cellular response is in early times of GE and LPS treatments, analysing both mRNA and protein levels. Jun is a TF member of the AP-1 complex, involved in various processes, i.e., cell proliferation, differentiation, apoptosis, stress response, inflammation, tumour suppression. Jun activity is regulated both at transcriptional level and especially at protein level through its phosphorylation (Meng & Xia, 2011). To account for the unexpected increase in Jun mRNA levels only in GE100 + LPS cells, we hypothesized that this dose of GE together with LPS triggers the transcription of Jun, as more protein may be needed to cope with LPS-induced inflammation. A similar result was also observed for HO-1 and Arg-1 mRNAs, which significantly increased only in GE100 + LPS cells, suggesting a possible link among these proteins. Consistently, Jun appeared connected to HO-1 (Hmox1) and Arg-1 from our STRING analysis, whose interactions resulted from annotated databases, co-expression and textmining (Fig. 9). It is known that AP-1 proteins are involved in HO-1 gene regulation in different cell types (Medina et al., 2020).

HO-1 is a stress-inducible and redox-sensitive enzyme, essential in the heme catabolism, known to play an important role in response to inflammation and oxidative stress, as it has been described as a cytoprotective, anti-inflammatory, detoxifying and therapeutics (Gozzelino

et al., 2010; Mandal et al., 2016). A series of plant-derived chemicals (curcumin, resveratrol) have been reported to induce HO-1 in different cell types, which then mediates their antioxidant properties (Abuarqoub et al., 2006).

The enzyme Arg-1, a critical regulator of innate/adaptive immune responses, is involved in arginine metabolism. From literature data, it appears that both HO-1 and Arg-1 could attenuate inflammatory response through inhibition of the pro-inflammatory cytokines/chemokines production (IL-1 β , IL-6) (Jeong et al., 2016; Lee et al., 2003), and of iNOS expression (Abuarqoub et al., 2006). We found that the elevated levels of HO-1 and Arg-1 mRNAs observed only in GE100 + LPS cells correlated with decreased expression of iNOS, IL-1 α , IL-6, IL-10, and TNF- α under the same conditions, consistent with the suggested anti-inflammatory action exerted by GE. Arg-1 competes with iNOS for the same substrate L-arginine, generating ornithine or nitric oxide (NO) respectively, thus affecting inflammatory responses in opposite ways. The induced expression of iNOS fulfils several functions in the organism, with beneficial effects, i.e., antiviral, bactericidal, immunomodulatory, antitumor. Indeed, improper iNOS induction, either in place or time, can have detrimental effects for the organism (Kleinert et al., 2004). The increased levels of iNOS mRNA induced by both doses might suggest GE hypothetical beneficial immunomodulatory effect in cells. Conversely, the drastic decrease of iNOS mRNAs in LPS-stimulated cells by GE50 pre-treatment could indicate an effective action of GE against harmful production of NO, although here we did not measure the presence, if any, of NO in the cells.

Cytokines are soluble mediators of intercellular signalling and communication, with biological activities in inflammation, immune response, cancer (Altan-Bonnet & Mukherjee, 2019). Among them, interleukins (IL) is a family of immune system regulators, primarily involved in immune cell differentiation and activation. IL-1 α is a major apical driver of many inflammatory processes, whereas IL-6 is a pleiotropic cytokine with pro/anti-inflammatory effects, acting also in many physiological events, e.g., gene activation, cell proliferation, survival, differentiation (Malik & Kanneganti, 2018; Tanaka et al., 2014). TNF- α has an important role comprising the pro-inflammatory response both locally and in circulation (Zlotnik & Yoshie, 2011). IL-10 is an anti-inflammatory cytokine, whose major function is to suppress macrophage production of pro-inflammatory cytokines, as TNF- α and IL-6 (Conti et al., 2003). Light/Tnfsf14, a member of the TNF ligand family, is known to stimulate T-cells proliferation and responses, and to trigger apoptosis of various cells (Tamada et al., 2000). Light/Tnfsf14 is pro-inflammatory in several contexts but can have a role in protection from intestinal inflammation (Giles et al., 2018). Considering the opposing roles reported for Light/Tnfsf14, its increased levels after all treatments, i.e., both doses of GE, LPS and GE50/100 + LPS, remains enigmatic.

MIF is a pro-inflammatory lymphokine with a putative role as regulator of the innate immune response, involved in host defence system against bacterial pathogens (Calandra & Roger, 2003). MIF is constitutively expressed by immune cells, rapidly released into tissues and/or circulation upon stimulation with LPS, although the production of high levels of MIF can be harmful during acute infections. The low levels of MIF mRNA found in all treatments, confirm that there wasn't its new transcription, consistent with the fact that high levels of MIF mRNA are constitutively present in cells (Calandra & Roger, 2003).

We observed the simultaneous expression of pro-/anti-inflammatory markers in LPS-stimulated cells. The balance between pro/anti-inflammatory responses, and the gene expression of the related cytokines, is quite regulated, and there is often a timing overlap in cytokine mRNA levels during immune response. This balance is truly dynamic and the immune system responds by maintaining a steady state level through continuous feedback with other immune molecules that mediate the balance over time (Cicchese et al., 2018). The deregulation of the immune response is instead characterized by an aggressive pro-inflammatory response combined with an anti-inflammatory one,

with a massive increase of the levels of several cytokines, as observed very recently also in COVID-19 inflammation (Notz et al., 2020; Tisoncik et al., 2012).

TRIB3 is considered an important marker of the ER oxidative stress, although its expression was shown to be also induced in response to diverse types of cellular stress (Ord & Ord, 2017). It is known to physically interact with TFs and kinases, and can function to promote/suppress cell death, depending on the cell and stress type. TRIB3 was related to TNF- α , IL-6, HO-1 (Hmox1), Rel-A and Jun by STRING analysis (Fig. 9). The increased levels of its mRNA induced by GE100, LPS and GE100 + LPS can be explained as a cellular defence mechanism, in order not to undergo apoptosis (Shimizu et al., 2012).

Pre-treatment of RAW264.7 with commercial [6]-gingerol produced similar results to pre-treatments with GE, as it was as effective as GE50 (TNF- α , iNOS) or GE100 (IL-1- α , IL-6, IL-10, Arg-1, TRIB3) in modifying LPS effects on mRNAs expression. We have previously shown that pre-treatment with commercial [6]-gingerol modulated the LPS-induced immune response also in immune cells of adult sea urchin, a marine organism used as model system in toxicology studies (Chiaramonte et al., 2021). Overall, the results shown here suggest that the observed GE effects can be mainly attributed to [6]-gingerol and that the other compounds constituting GE, although not yet characterized here, would probably not alter its effectiveness. More than one of the single components of ginger can have anti-inflammatory effects, other than [6]-gingerol. For example, [6]-shogaol can attenuate inflammation inhibiting AP-1 and NF- κ B TFs in hamsters carcinogenesis (Annamalai & Suresh, 2018), reduce LPS-induced inflammation via Cox2/iNOS inhibition both in murine microglia BV-2 and RAW264.7 cells, reduce TNF- α and IL-1 β LPS-induced expression in RAW264.7 (Bischoff-Kont & Fürst, 2021). At present, with the available data, we cannot determine whether other members of GE may have played a role in the observed effects.

Macrophages can be found as two main phenotypes, resulting from a specific polarization process, influenced by the local tissue environment (Sica & Mantovani, 2012). Classically (M1) and alternatively (M2) activated macrophages represent extremes of several intermediate activated states, producing cytokines according to their phenotypes, although a clear-cut distinction may not exist and overlapping effects may be present (Wang et al., 2019). It has been suggested that M1/M2 polarity arises from arginine metabolism via two antagonistic pathways: M1-like phenotype is the product of iNOS pathway, whereas M2-like phenotype is the product of arginase pathway. Therefore, iNOS and Arg-1 genes are widely used as markers for the characterization of M1 and M2 phenotype, respectively (Yang & Ming, 2014), although the best strategy to discriminate between different phenotypes seems to be the combination of different markers, as some can be expressed by multiple cell types (Wang et al., 2019). From our results, we can assume that GE does not activate any macrophage phenotype used alone. LPS treatment, increasing mRNA levels of iNOS and all the analysed cytokines but not those of Arg-1, likely activates M1-like phenotype, which has a pro-inflammatory activity. Contrarily, the reduced levels of iNOS, significant increase of Arg-1, and high levels of Light/Tnfsf14 in GE100 + LPS cells suggest a trend towards the activation of a M2-like phenotype, with known anti-inflammatory functions. However, more in-depth studies are needed to understand what the real scenario is.

5. Conclusion

Inflammation and oxidative stress are major contributors to the development of many pathological states, and it is remarkable that a diet rich in antioxidants can effectively reduce the risk of developing them. Foods exhibiting anti-inflammatory properties, such as vegetables and a variety of phytochemicals, appear to provide significant benefit when consumed regularly, activating protective mechanisms useful for therapeutic applications.

Although many studies on bioactive molecules are present in the literature, they are still not conclusive, especially concerning dosages,

bioavailability, metabolism, and interaction with other components of nutritional interest. Thus, further extensive research is important to manage the use of medicinal plants and/or their derivatives in the modern medicine.

This study intends to highlight the features of a new total ethanol extract from ginger, in comparison with the commercial [6]-gingerol, analysing its anti-inflammatory/antioxidant properties on RAW264.7 and evaluating the effects obtained with respect to macrophage M1/M2 polarization. Certainly, further analyses are needed to better understand the role of individual components present in our GE, with the aim of understanding whether a synergistic effect among them may be present. In the long term, the aim would be to provide a pharmacological basis for the treatment of inflammatory diseases.

Author statement

All authors take public responsibility for the content of the work submitted for review.

The authors confirm contribution to the paper as follows: RR, MC, FZ, NL and MAC designed the study; AP, MRM, MC, RR, FZ performed experiments; RR, FZ, NL and MAC wrote the paper; RP contributed to write the paper by revising it critically.

All authors reviewed the results and approved the final version of the manuscript.

Declaration of competing interest

The authors declare that they have no known competing financial interests or personal relationships that could have appeared to influence the work reported in this paper.

Data availability

No data was used for the research described in the article.

Acknowledgements

We thank the project P.O.FSE 2014/2020 “Rafforzare l’occupabilità nel sistema r&s e la nascita di spin off di ricerca in Sicilia”. CUP: G77B17000220009; CIP: 2014.IT.05.SFOP.014/3/10.4/9.2.10/0013.

Appendix A. Supplementary data

Supplementary data to this article can be found online at <https://doi.org/10.1016/j.fbio.2023.102746>.

References

- Abuqarqub, H., Foresti, R., Green, C. J., & Motterlini, R. (2006). Heme oxygenase-1 mediates the anti-inflammatory actions of 2'-hydroxychalcone in RAW 264.7 murine macrophages. *American Journal of Physiology - Cell Physiology*, 290(4), 1092–1099. <https://doi.org/10.1152/ajpcell.00380.2005>
- Ali, A. M. A., El-Nour, M. E. A. M., & Yagi, S. M. (2018). Total phenolic and flavonoid contents and antioxidant activity of ginger (*Zingiber officinale* Rosc.) rhizome, callus and callus treated with some elicitors. *Journal of Genetic Engineering and Biotechnology*, 16(2), 677–682. <https://doi.org/10.1016/j.jgeb.2018.03.003>
- Altan-Bonnet, G., & Mukherjee, R. (2019). Cytokine-mediated communication: A quantitative appraisal of immune complexity. *Nature Reviews Immunology*, 19(4), 205–217. <https://doi.org/10.1038/s41577-019-0131-x>
- Annamalai, G., & Suresh, K. (2018). [6]-Shogaol attenuates inflammation, cell proliferation via modulate NF- κ B and AP-1 oncogenic signaling in 7,12-dimethylbenz[a]anthracene induced oral carcinogenesis. *Biomedicine & Pharmacotherapy*, 98, 484–490. <https://doi.org/10.1016/j.biopha.2017.12.009>
- Ballester, P., Cerdá, B., Arcusa, R., Marhuenda, J., Yamedjeu, K., & Zafrilla, P. (2022). Effect of ginger on inflammatory diseases. *Molecules*, 27(21). <https://doi.org/10.3390/molecules27217223>
- Bischoff-Kont, I., & Fürst, R. (2021). Benefits of ginger and its constituent 6-shogaol in inhibiting inflammatory processes. *Pharmaceuticals*, 14(6), 1–19. <https://doi.org/10.3390/ph14060571>

- Calandra, T., & Roger, T. (2003). Macrophage migration inhibitory factor: A regulator of innate immunity. *Nature Reviews Immunology*, 3(10), 791–800. <https://doi.org/10.1038/nri1200>
- Chiaramonte, M., Bonaventura, R., Costa, C., Zito, F., & Russo, R. (2021). [6]-Gingerol dose-dependent toxicity, its role against lipopolysaccharide insult in sea urchin (*Paracentrotus lividus* Lamarck), and antimicrobial activity. *Food Bioscience*, 39. <https://doi.org/10.1016/j.fbio.2020.100833>. March 2020.
- Cicchese, J. M., Evans, S., Hult, C., Joslyn, L. R., Wessler, T., Millar, J. A., Marino, S., Cilfone, N. A., Mattila, J. T., Linderman, J. J., & Kirschner, D. E. (2018). Dynamic balance of pro- and anti-inflammatory signals controls disease and limits pathology. *Immunological Reviews*, 285(1), 147–167. <https://doi.org/10.1111/immr.12671>
- Conti, P., Kempuraj, D., Kandere, K., Gioacchino, M. Di, Barbacane, R. C., Castellani, M. L., Felaco, M., Boucher, W., Letourneau, R., & Theoharides, T. C. (2003). IL-10, an inflammatory/inhibitory cytokine, but not always. *Immunology Letters*, 86(2), 123–129. [https://doi.org/10.1016/S0165-2478\(03\)00002-6](https://doi.org/10.1016/S0165-2478(03)00002-6)
- Dávalos, A., Gómez-Cordovés, C., & Bartolomé, B. (2004). Extending applicability of the oxygen radical absorbance capacity (ORAC-fluorescein) assay. *Journal of Agricultural and Food Chemistry*, 52(1), 48–54. <https://doi.org/10.1021/jf0305231>
- De Sanctis, B. H., Moreira, F., & Toledo Cerqueira, C. (2022). Action of bioactive compounds on inflammation via nuclear factor-kappa B in chronic noncommunicable diseases - insights for neuropsychiatric disorders. *Acta Scientifi Nutritional Health*, 6(12), 71–81. <https://doi.org/10.31080/asnh.2022.06.1155>
- Giles, D. A., Zahner, S., Krause, P., Van Der Gracht, E., Riffelmacher, T., Morris, V., Tumanov, A., & Kronenberg, M. (2018). The tumor necrosis factor superfamily members TNFSF14 (LIGHT), lymphotxin β and lymphotxin β receptor interact to regulate intestinal inflammation. *Frontiers in Immunology*, 9, 1–9. <https://doi.org/10.3389/fimmu.2018.02585>. NOV.
- Gozzelino, R., Jeney, V., & Soares, M. P. (2010). Mechanisms of cell protection by heme Oxygenase-1. *Annual Review of Pharmacology and Toxicology*, 50, 323–354. <https://doi.org/10.1146/annurev.pharmtox.010909.105600>
- Gutfinger, T. (1981). Polyphenols in olive oils. *Journal of the American Oil Chemists Society*, 58(11), 966–968. <https://doi.org/10.1007/BF02659771>
- Ho, S.-C., Chang, K.-S., & Lin, C.-C. (2013). Anti-neuroinflammatory capacity of fresh ginger is attributed mainly to 10-gingerol. *Food Chemistry*, 141(3), 3183–3191. <https://doi.org/10.1016/j.foodchem.2013.06.010>
- Hossain, M. B., Barry-Ryan, C., Martin-Diana, A. B., & Brunton, N. P. (2010). Effect of drying method on the antioxidant capacity of six Lamiaceae herbs. *Food Chemistry*, 123(1), 85–91. <https://doi.org/10.1016/j.foodchem.2010.04.003>
- Jeong, S. J., Kim, O. S., Yoo, S. R., Seo, C. S., Kim, Y., & Shin, H. K. (2016). Anti-inflammatory and antioxidant activity of the traditional herbal formula Gwakhkyangjeonggi-san via enhancement of heme oxygenase-1 expression in RAW264.7 macrophages. *Molecular Medicine Reports*, 13(5), 4365–4371. <https://doi.org/10.3892/mmr.2016.5084>
- Jones, D. P. (2002). Redox potential of GSH/GSSG couple: Assay and biological significance. *Methods in Enzymology*, 348, 93–112. [https://doi.org/10.1016/s0076-6879\(02\)48630-2](https://doi.org/10.1016/s0076-6879(02)48630-2)
- Karin, M., Hawkins, P. T., Irvine, R. F., Michell, R. H., & Marshall, C. J. (1996). The regulation of AP-1 activity by mitogen-activated protein kinases. *Philosophical Transactions of the Royal Society of London - Series B: Biological Sciences*, 351(1336), 127–134. <https://doi.org/10.1098/rstb.1996.0008>
- Kawai, T., & Akira, S. (2007). Signaling to NF-kappaB by toll-like receptors. *Trends in Molecular Medicine*, 13(11), 460–469. <https://doi.org/10.1016/j.molmed.2007.09.002>
- Kawai, T., & Akira, S. (2010). The role of pattern-recognition receptors in innate immunity: Update on toll-like receptors. In *Nature immunology*. <https://doi.org/10.1038/ni.1863>
- Kleinert, H., Pautz, A., Linker, K., & Schwarz, P. M. (2004). Regulation of the expression of inducible nitric oxide synthase. *European Journal of Pharmacology*, 500(1–3), 255–266. <https://doi.org/10.1016/j.ejphar.2004.07.030>
- Lawrence, T. (2009). The nuclear factor NF-kappaB pathway in inflammation. *Cold Spring Harbor Perspectives in Biology*, 1(6), a001651. <https://doi.org/10.1101/cshperspect.a001651>
- Lee, T.-S., Tsai, H.-L., & Chau, L.-Y. (2003). Induction of heme oxygenase-1 expression in murine macrophages is essential for the anti-inflammatory effect of low dose 15-Deoxy- Δ 12,14-prostaglandin J2. *Journal of Biological Chemistry*, 278(21), 19325–19330. <https://doi.org/10.1074/jbc.M300498200>
- Liang, N., Sang, Y., Liu, W., Yu, W., & Wang, X. (2018). Anti-inflammatory effects of gingerol on lipopolysaccharide-stimulated RAW 264.7 cells by inhibiting NF- κ B signaling pathway. *Inflammation*, 41(3), 835–845. <https://doi.org/10.1007/s10753-018-0737-3>
- Li, F., Nitteranon, V., Tang, X., Liang, J., Zhang, G., Parkin, K. L., & Hu, Q. (2012). In vitro antioxidant and anti-inflammatory activities of 1-dehydro-[6]-gingerdione, 6-shogaol, 6-dehydroshogaol and hexahydrocurcumin. *Food Chemistry*, 135(2), 332–337. <https://doi.org/10.1016/j.foodchem.2012.04.145>
- Liu, F., Zhang, X., Ling, P., Liao, J., Zhao, M., Mei, L., Shao, H., Jiang, P., Song, Z., Chen, Q., & Wang, F. (2017). Immunomodulatory effects of xanthan gum in LPS-stimulated RAW 264.7 macrophages. *Carbohydrate Polymers*, 169, 65–74. <https://doi.org/10.1016/j.carbpol.2017.04.003>
- Malik, A., & Kanneganti, T. D. (2018). Function and regulation of IL-1 α in inflammatory diseases and cancer. *Immunological Reviews*, 281(1), 124–137. <https://doi.org/10.1111/immr.12615>
- Mandal, C. C., Das, F., Ganapathy, S., Harris, S. E., Choudhury, G. G., & Ghosh-Choudhury, N. (2016). Bone morphogenetic protein-2 (BMP-2) activates NFATc1 transcription factor via an autoregulatory loop involving Smad/Akt/Ca2+ signaling. *Journal of Biological Chemistry*, 291(3), 1148–1161. <https://doi.org/10.1074/jbc.M115.668939>
- Mao, Q. Q., Xu, X. Y., Cao, S. Y., Gan, R. Y., Corke, H., Beta, T., & Li, H. B. (2019a). Bioactive compounds and bioactivities of ginger (*Zingiber officinale* roscoe). *Foods*, 8(6), 1–21. <https://doi.org/10.3390/Foods8060185>
- Mao, Q. Q., Xu, X. Y., Cao, S. Y., Gan, R. Y., Corke, H., Beta, T., & Li, H. B. (2019b). Bioactive compounds and bioactivities of ginger (*Zingiber officinale* roscoe). In *Foods* (Vol. 8)MDPI Multidisciplinary Digital Publishing Institute. <https://doi.org/10.3390/foods8060185>, 6.
- Martinez, F. O., & Gordon, S. (2014). The M1 and M2 paradigm of macrophage activation: Time for reassessment. *F1000Prime Reports*, 6(March), 1–13. <https://doi.org/10.12703/P6-13>
- Mashadi, N. S., Ghiasvand, R., A. G., H. M., D. L., & Mofid, M. R. (2013). Anti-oxidative and anti-inflammatory effects of ginger in health and physical activity: Review of current evidence. *International Journal of Preventive Medicine*, 36–42.
- Mazahery, H., Conlon, C. A., Beck, K. L., Mugridge, O., Kruger, M. C., Stonehouse, W., C. C. A., Jr., Meyer, B. J., Tsang, B., & Hurst, P. R. von (2019). Inflammation (IL-1 β) modifies the effect of vitamin D and omega-3 long chain polyunsaturated fatty acids on core symptoms of autism spectrum disorder. *Proceedings*, 37(1). <https://doi.org/10.3390/proceedings2019037002>
- Medina, M. V., Sapochnik, D., Garcia Solá, M., & Coso, O. (2020). Regulation of the expression of heme oxygenase-1: Signal transduction, gene promoter activation, and beyond. *Antioxidants and Redox Signaling*, 32(14), 1033–1044. <https://doi.org/10.1089/ars.2019.7991>
- Meng, Q., & Xia, Y. (2011). c-Jun, at the crossroad of the signaling network. *Protein and Cell*, 2(11), 889–898. <https://doi.org/10.1007/s13238-011-1113-3>
- Mozaffari-Khosravi, H., Talaei, B., Jalali, B.-A., Najarzadeh, A., & Mozayan, M. R. (2014). The effect of ginger powder supplementation on insulin resistance and glycemic indices in patients with type 2 diabetes: A randomized, double-blind, placebo-controlled trial. *Complementary Therapies in Medicine*, 22(1), 9–16. <https://doi.org/10.1016/j.ctim.2013.12.017>
- Mussbacher, M., Derler, M., Basilio, J., & Schmid, J. A. (2023). NF- κ B in monocytes and macrophages – an inflammatory master regulator in multitailed immune cells. *Frontiers in Immunology*, 14, 1–13. <https://doi.org/10.3389/fimmu.2023.1134661>. February.
- Mustafa, I., Chin, N. L., Fakurazi, S., & Palanisamy, A. (2019). Comparison of phytochemicals, antioxidant and anti-inflammatory properties of sun-, oven- and freeze-dried ginger extracts. *Foods*, 8(10). <https://doi.org/10.3390/foods8100456>
- Ninfali, P., Bacchiocca, M., Biagiotti, E., Servili, M., & Montedoro, G. (2002). Validation of the oxygen radical absorbance capacity (ORAC) parameter as a new index of quality and stability of virgin olive oil. *Journal of the American Oil Chemists' Society*, 79(10), 977–982. <https://doi.org/10.1007/s11746-002-0590-7>
- Notz, Q., Schmalzing, M., Wedekink, F., Schlesinger, T., Gernert, M., Herrmann, J., Sorger, L., Weismann, D., Schmid, B., Sitter, M., Schlegel, N., Kranke, P., Wischhusen, J., Meybohm, P., & Lotz, C. (2020). Pro- and anti-inflammatory responses in severe COVID-19-induced acute respiratory distress syndrome—an observational pilot study. *Frontiers in Immunology*, 11(October), 1–13. <https://doi.org/10.3389/fimmu.2020.581338>
- Ok, S., & Jeong, W. S. (2012). Optimization of extraction conditions for the 6-shogaol-rich extract from ginger (*Zingiber officinale* Roscoe). *Preventive Nutrition and Food Science*, 17(2), 166–171. <https://doi.org/10.3746/pnf.2012.17.2.166>
- Ord, T., & Ord, T. (2017). Mammalian Pseudokinase TRIB3 in normal physiology and disease: Charting the progress in old and new avenues. *Current Protein & Peptide Science*, 18(8), 819–842. <https://doi.org/10.2174/1389203718666170406124547>
- Park, E., Lee, C. G., Jeon, H., Jeong, H., Yeo, S., Yong, Y., & Jeong, S. Y. (2021). Anti-obesity effects of combined cornu officinalis and ribes fasciculatum extract in high-fat diet-induced obese male mice. *Animals*, 11(11), 1–13. <https://doi.org/10.3390/ani1113187>
- Poprac, P., Jomova, K., Simunkova, M., Kollar, V., Rhodes, C. J., & Valko, M. (2017). Targeting free radicals in oxidative stress-related human diseases. *Trends in Pharmacological Sciences*, 38(7), 592–607. <https://doi.org/10.1016/j.tips.2017.04.005>
- Qian, C., & Cao, X. (2013). Regulation of Toll-like receptor signaling pathways in innate immune responses. *Annals of the New York Academy of Sciences*, 1283, 67–74. <https://doi.org/10.1111/j.1749-6632.2012.06786.x>
- Serrano, A., Ros, G., & Nieto, G. (2018). Bioactive compounds and extracts from traditional herbs and their potential anti-inflammatory health effects. *Medicines (Basel, Switzerland)*, 5(3). <https://doi.org/10.3390/medicines5030076>
- Shimizu, K., Takahama, S., Endo, Y., & Sawasaki, T. (2012). Stress-inducible caspase substrate TRB3 promotes nuclear translocation of procaspase-3. *PLoS One*, 7(8), 1–13. <https://doi.org/10.1371/journal.pone.0042721>
- Shim, S., Kim, S., Choi, D.-S., Kwon, Y.-B., & Kwon, J. (2011). Anti-inflammatory effects of [6]-shogaol: Potential roles of HDAC inhibition and HSP70 induction. *Food and Chemical Toxicology*, 49(11), 2734–2740. <https://doi.org/10.1016/j.fct.2011.08.012>
- Sica, A., & Mantovani, A. (2012). Science in medicine macrophage plasticity and polarization : In vivo veritas. *Journal of Clinical Investigation*, 122(3), 787–795. <https://doi.org/10.1172/JCI59643DS1>
- Sung, M. H., Li, N., Lao, Q., Gottschalk, R. A., Hager, G. L., & Fraser, I. D. C. (2014). Switching of the relative dominance between feedback mechanisms in lipopolysaccharide-induced NF- κ B signaling. *Science Signaling*, 7(308). <https://doi.org/10.1126/scisignal.2004764>
- Szklarczyk, D., Kirsch, R., Koutrouli, M., Nastou, K., Mehryary, F., Hachilif, R., Gable, A. L., Fang, T., Doncheva, N. T., Pyysalo, S., Bork, P., Jensen, L. J., & von Mering, C. (2023). The STRING database in 2023: Protein-protein association networks and functional enrichment analyses for any sequenced genome of interest. *Nucleic Acids Research*, 51(D1), D638–D646. <https://doi.org/10.1093/nar/gkac1000>
- Tamada, K., Shimozaki, K., Chapoval, A. I., Zhai, Y., Su, J., Chen, S.-F., Hsieh, S.-L., Nagata, S., Ni, J., & Chen, L. (2000). LIGHT, a TNF-like molecule, costimulates T cell

- proliferation and is required for dendritic cell-mediated allogeneic T cell response. *The Journal of Immunology*, 164(8), 4105–4110. <https://doi.org/10.4049/jimmunol.164.8.4105>
- Tanaka, T., Narazaki, M., & Kishimoto, T. (2014). IL-6 in inflammation, immunity, and disease. *Cold Spring Harbor Perspectives in Biology*, 6(10), a016295. <https://doi.org/10.1101/cshperspect.a016295>
- Tisoncik, J. R., Korth, M. J., Simmons, C. P., Farrar, J., Martin, T. R., & Katze, M. G. (2012). Into the eye of the cytokine storm. *Microbiology and Molecular Biology Reviews*, 76(1), 16–32. <https://doi.org/10.1128/mmb.05015-11>
- Wang, L. xun, Zhang, S., xi, W., juan, H., Rong, X. lu, & Guo, J. (2019). M2b macrophage polarization and its roles in diseases. *Journal of Leukocyte Biology*, 106(2), 345–358. <https://doi.org/10.1002/JLB.3RU1018-378RR>
- Yang, Z., & Ming, X. F. (2014). Functions of arginase isoforms in macrophage inflammatory responses: Impact on cardiovascular diseases and metabolic disorders. *Frontiers in Immunology*, 5, 1–10. <https://doi.org/10.3389/fimmu.2014.00533>. OCT.
- Zlotnik, A., & Yoshie, O. (2011). The chemokine superfamily revisited NIH public access. *Bone*, 23(1), 1–7. <https://doi.org/10.1016/j.immuni.2012.05.008>, 19, (The).